Semaan, Patricia; Zahran, Abraham; Schlapp-Hackl, Inge; Tehrani-Bagha, Ali R.; Mustapha, Samir

Enhanced mechanical properties of epoxy composites using cellulose micro- and nano-crystals

Published in:
Journal of Applied Polymer Science

DOI:
10.1002/app.55180

Published: 10/04/2024

Document Version
Publisher's PDF, also known as Version of record

Please cite the original version:
Semaan, P., Zahran, A., Schlapp-Hackl, I., Tehrani-Bagha, A. R., & Mustapha, S. (2024). Enhanced mechanical properties of epoxy composites using cellulose micro- and nano-crystals. *Journal of Applied Polymer Science*, *141*(14), Article e55180. https://doi.org/10.1002/app.55180

Received: 31 August 2023 | Revised: 21 December 2023 | Accepted: 27 December 2023

DOI: 10.1002/app.55180

RESEARCH ARTICLE

Journal of Applied Polymer Science WILEY

Enhanced mechanical properties of epoxy composites using cellulose micro- and nano-crystals

Patricia Semaan[1] | **Abraham Zahran**[1] | **Inge Schlapp-Hackl**[2] | **Ali R. Tehrani-Bagha**[2] | **Samir Mustapha**[3]

[1]B. & W. Bassatne Department of Chemical Engineering and Advanced Energy, American University of Beirut, Beirut, Lebanon

[2]Department of Bioproducts and Biosystems, Aalto University, Espoo, Finland

[3]Department of Mechanical Engineering, American University of Beirut, Beirut, Lebanon

Correspondence
Ali R. Tehrani-Bagha, Department of Bioproducts and Biosystems, Aalto University, Espoo, Finland.
Email: ali.tehrani@aalto.fi

Samir Mustapha, Department of Mechanical Engineering, American University of Beirut, Beirut, Lebanon.
Email: sm154@aub.edu.lb

Funding information
University Research Board at the American University of Beirut, Grant/Award Number: 104260

Abstract

Epoxy polymers are commonly utilized in structural applications due to their high bearing capacity and excellent chemical resistance. However, their inherent brittleness poses a significant challenge for their use in high shock and fracture strength products. To address this shortcoming, fillers can be incorporated into the polymer during preparation. In this study, we aimed to investigate the effect of incorporating cellulose-based fillers, namely cellulose nanocrystals (CNCs) and microcrystalline cellulose (MCC), on the mechanical properties of epoxy polymer composites. The study evaluated the impact of various factors, including filler concentration, particle size, and moisture content, on the mechanical properties of the composites. The results demonstrated that the incorporation of CNC or MCC powders at concentrations below 5% could enhance the mechanical properties of the resulting epoxy composites without adversely affecting their surface and thermal properties. The maximum tensile strength and fracture toughness of the filler-based epoxy composites were achieved at 2 and 4 wt% for CNCs and MCC, respectively. CNCs with a smaller particle size distribution were found to be much more effective than MCC in improving the mechanical properties of the epoxy composites. Furthermore, utilizing dried fillers resulted in a higher improvement in tensile strength, which was achieved at lower filler concentrations.

KEYWORDS

epoxy composite, filler water content, mechanical properties, microcrystalline cellulose, nanocrystalline cellulose

1 | INTRODUCTION

Epoxy-based composites with high mechanical properties and stability are used in the automotive, appliances, energy, and electrical industry.[1,2] The epoxy group is known for its reactivity to nucleophilic and electrophilic species, making epoxy polymers receptive to a broad range of curing agents (i.e., hardeners). Common examples of hardeners include aliphatic and aromatic amines, carboxylic anhydrides, and imides. The hardener reacts with epoxy resin through the epoxide group to cross-link and form a 3D network structure.[3] Epoxy polymers are used in various fields such as adhesives, surface coatings, and composites. Based on curing kinetics and chemical compositions, it is possible to adjust their mechanical properties ranging from intense flexibility to high potency and hardness. However, extensive use of epoxy thermosets in several high-potential applications is restricted due to their delamination, brittleness, and fracture toughness limitations.[4]

The properties of polymers can be improved by adding fillers of different types, sizes, and shapes.[5,6] This will enhance their properties and widen their applications. Nevertheless, the reinforcement mostly depends on the filler's physical and chemical properties such as type, quantity, dispersion, and interaction of the filler with the polymer.[7] The fillers can be classified into two large groups of (i) inorganic metal oxides containing zinc, iron, copper, and aluminum and (ii) organic fillers including fullerenes, carbon black, carbon nanotubes, graphene, and their derivatives. These fillers have often been used to enhance the mechanical properties of epoxy resin, namely, tensile strength and fracture toughness. As good examples, one can increase the tensile strength of epoxy composites by 20%–25% by adding 0.5 wt% of nanosilica[8,9] or 0.5 wt% graphitic carbon nitride (g-C_3H_4).[10]

Microcrystalline cellulose (MCC) and cellulose nanocrystals (CNCs) are separated fragments of cellulose that exhibit variations in size, morphology, crystallinity, and structure. MCC and CNCs have gained attention for their use as reinforcing agents/fillers in polymer-based composites.[11] Both fillers share common features such as high crystallinity and stability, good mechanical properties, high surface area, and abundant active surface groups.[12] In particular, the hydroxyl groups present in MCC and CNCs can undergo countless chemical modifications, making them more appealing as reinforcing fillers.[13]

A few research studies investigated the reinforcing effect of adding MCC and CNCs to thermosetting and thermoplastic polymers to improve their mechanical properties. By increasing the amount of filler, the mechanical tensile strength of the resulting composites increased, reaching a maximum at a certain filler concentration.[14] Beyond this concentration, adding more filler would decrease the tensile strength due to filler agglomeration. This was observed in a study when 0.125, 0.25, 0.5, and 1 wt% of CNCs were added to epoxy resin. The optimal value for tensile strength was obtained at 0.25 wt% of CNC.[15] The addition of filler beyond this concentration reduced the polymer's mechanical properties due to filler agglomeration.[14–18] Moreover, the addition of the fillers with different types of polymers showed how the fillers' reinforcement was also affected by the interaction and compatibility of the polymer with the filler. To enhance the compatibility between fillers and polymer matrix, one can modify the surface properties of fillers. This will enhance the properties of the resulting polymer composites.[19–21] In one study, hyper-branched aromatic polyamide grown on MCC fibers was added to epoxy to induce a stronger affinity between the matrix and the filler, and this increases the tensile strength of the composite by 34.7%.[22] The second approach to enhance the mechanical properties of epoxy composites is to use a less viscous hardener with a higher number of amine groups to disperse CNCs in the matrix better.[23]

Because of the presence of several hydroxyl groups and owing to their hydrophilic nature, CNCs and MCC are hygroscopic, meaning they can absorb moisture. As such, the presence of water can interfere with the reaction between the epoxy monomer and the hardener by terminating the polymerization and preventing the formation of a well-established 3D network. They can also be entrapped in the matrix and generate weak points and stress concentrations. During the curing process, some studies showed how excess water can alter curing kinetics and may solubilize some components like the amine hardener at high concentrations (e.g., 6 wt%) thereby reducing the contact between the epoxy and the hardener and slowing down the reaction and creating barriers that inhibit the epoxy molecules from making bonds.[24,25] Another study points out the degradation in mechanical properties of epoxy resins, namely tensile strength and stiffness, through a plasticization phenomenon due to moisture exposure.[26]

Previous research has demonstrated that moisture can have a negative impact on the interface between matrix and filler, resulting in debonding and reduced mechanical properties, including tensile strength.[27,28] The presence of water molecules can also cause poor interaction between fibers and matrix due to hydrogen bonding. As a result, the bonding between the filler and polymer matrix can be compromised, leading to filler agglomeration. Additionally, intra- and inter-molecular hydrogen bonding in cellulosic particles can be promoted by water, which exacerbates the poor interfacial adhesion between filler and matrix.[29]

Several studies have explored the impact of CNC reinforcement on epoxy composites, revealing promising improvements in mechanical and thermal properties. For instance, investigations utilizing triethylenetetramine as a curing agent demonstrated notable increases in tensile strength and elastic modulus, peaking at 1 wt% CNC.[30] In another study, which examined crystalline nanocrystals and fibers, substantial enhancements in elastic modulus, tensile strength, and fracture toughness were

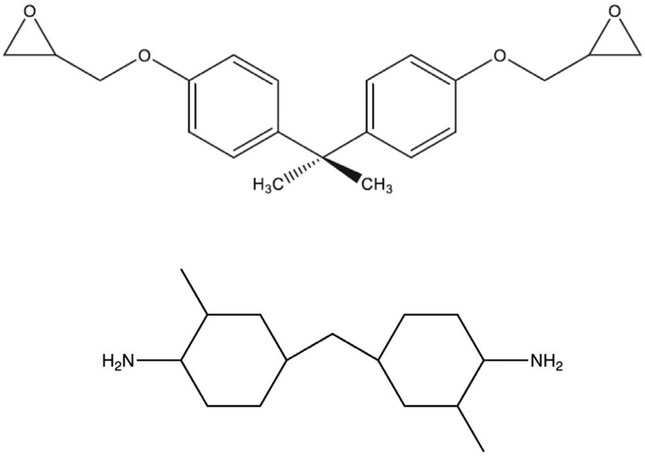

FIGURE 1 Araldite LY 564 epoxy resin chemical structure (top) and Aradur 2954 hardener chemical structure (bottom).[33]

observed with the addition of a high concentration of CNCs around 16.7 wt%.[31] The incorporation of modified CNCs at 0.5 wt% resulted in significant improvements in tensile strength, modulus, and thermal stability.[32]

To address gaps in previous research, our study investigates the effects of both CNCs and MCC on epoxy composites using consistent epoxy components and preparation conditions. We introduce a novel dimension by examining the impact of oven drying MCC and CNC before epoxy composite preparation, offering insights into their reinforcing effects before and after the drying process. The focus of our study on diverse cellulose fillers and the influence of drying constitutes a novel contribution to understanding the thermo-mechanical properties of epoxy composites.

2 | METHODOLOGY

2.1 | Materials

Epoxy resin "Araldite LY 564" and the cycloaliphatic polyamine hardener "Aradur 2954" were purchased from "Huntsman Inc" and used during the preparation of the composite materials. Their chemical structures can be seen in Figure 1, respectively. When these chemicals are mixed, the epoxy resin undergoes an exothermic addition reaction, which yields a completely cured and cross-linked 3D network.[8,9]

Pure CNCs were purchased from CelluForce-Canada, which according to the data-sheet is a re-dispersible powder of uniform acyclic nanometric crystals with a particle size of less than 150 nm. Spray-dried MCC of 95.6% dry matter content was kindly provided by Nordic Bioproducts Group Oy-Finland.

2.2 | Preparation of composites

2.2.1 | Preparing epoxy composites

For preparing epoxy polymer samples, the epoxy resin and the hardener (Figure 1) should be mechanically mixed first. The mixture is then poured inside molds and cured at a high temperature (typically 140°C). We tried different methods for adding the filler to the matrix of epoxy composite (e.g., adding the filler to epoxy resin first, adding the filler to the hardener first, and dispersing the filler in acetone mixing it with the hardener). After several screening tests, we found that the best practice for adding the filler to the epoxy matrix is by initially mixing the filler with the hardener without adding any solvent. The sample preparation of the epoxy composite has been schematically shown in Figure 2.

The procedure for preparing the epoxy composites is as follows: CNC powder was first added to the hardener and mechanically stirred for 10 min. The mixture was then sonicated for 30 min using Elma ultrasonic cleaner S80H. The mixture was left to cool for 5 min, and then the epoxy was added and mechanically stirred until the mixture became homogeneous. The mixture was then degassed for 2 h in a vacuum oven (model OV-12) at −0.1 MPa vacuum and was subsequently poured into aluminum molds (Figure 3). The molds containing the mixture were placed in the vacuum oven to be degassed for 2.5 h. The molds were then preheated at 80°C an hour and cured at 140°C for 8 h. After curing, each sample was removed from the mold and polished manually using P100 and P400 sandpapers.

2.2.2 | Drying procedure for fillers

To understand the effect of filler moisture content, it was essential to study how the removal of moisture from the fillers can affect the final composite's properties. CNC and MCC powders were dried in an oven at 110°C for 24 h to eliminate adsorbed water, following the procedure outlined in previous research.[34] Upon oven drying the filler, the hot containers containing dried powders were put in a desiccator to cool to avoid recapturing moisture from the environment. The moisture content of the CNC and MCC samples was found to be around 7% by the weight loss%.

2.3 | Characterization of CNCs and MCC

2.3.1 | Dynamic light scattering analysis

Q2000 dynamic light scattering (DLS) was used to determine the particle size of MCC and CNC powders dispersed in different solvents. The dispersions in water,

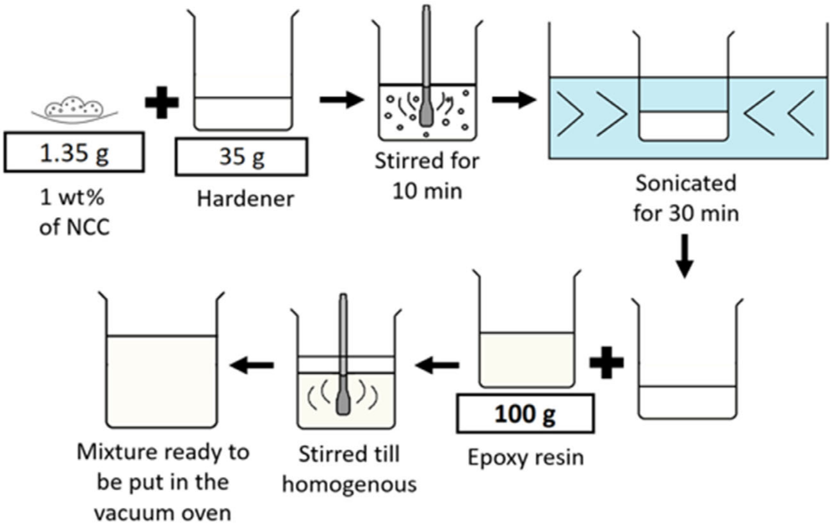

FIGURE 2 Schematic of the general procedure for preparing epoxy composite using the optimal method of mixing cellulose nanocrystals with hardener first. [Color figure can be viewed at wileyonlinelibrary.com]

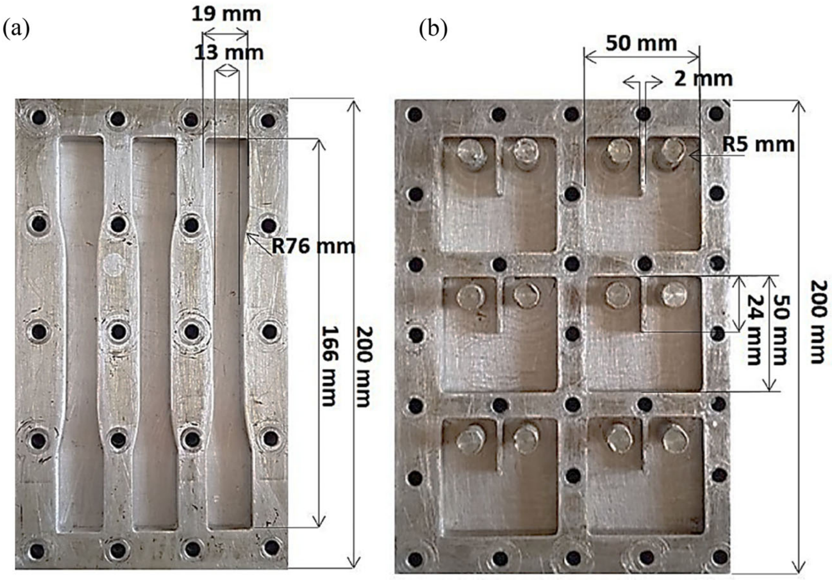

FIGURE 3 (a) The dimensions of the molds for preparing the dog-bone samples for the mechanical tensile test, (b) the dimensions of the mold for the compact tension test. [Color figure can be viewed at wileyonlinelibrary.com]

ethanol, and dimethylformamide (DMF) in the range of 0.25–0.5 wt% were sonicated for 3 min and transferred to a 2 mL cuvette for DLS analysis. The particle size distribution of the dispersions was measured 10 times to report the average and standard deviation.

2.3.2 | X-ray diffractometer

The x-ray diffractometer Xenocs Xeuss 3.0 equipped with a 2D Dectris Eiger2 R 1M detector (sample-to-detector distance: 56 mm) was used for determining the crystallinity index (CI) and the cellulose polymorphs of the MCC and CNC powders. The instrument was operated with CuK$_\alpha$ radiation in transmission mode at 50 kV and 0.6 mA at a wavelength of 1.54189 Å. The powders were fixed to the sample holder with kapton tape. A blank run (kapton tape without any sample) was performed to correct the scattering profiles. The sample profiles were illustrated via Origin.[34] The Segal CI % was calculated according to[35] by the following equation:

$$\mathrm{CI\%} = \frac{(I_{\mathrm{total}} - I_{\mathrm{amorphous}})}{I_{\mathrm{total}}} \times 100, \quad (1)$$

where I_{total} is the total intensity at 22° 2θ, and $I_{\mathrm{amorphous}}$ is the intensity at 18° 2θ for cellulose I.

2.4 | Characterization of epoxy

2.4.1 | Mechanical tensile testing and compact tension of composites

A universal mechanical testing machine was used to perform the mechanical tensile testing according to the standard test method ASTM D638. A laser extensometer measured the strain with a 100 kN load cell and a 1 mm/min loading rate. The dog-bone samples had a gauge length of about 50 mm with a cross-sectional area of 13 × 7 mm^2. A minimum of five samples was tested for each batch.

The mechanical testing machine was used for testing the compact tension of the square samples with a 100 kN load cell and a crosshead speed of 0.5 mm/min. The square samples of 40 mm × 40 mm with a thickness of 10 mm and a 24 mm notch in the middle of the sample were prepared according to the ASTM standard D5045 (Figure 3). To conduct the test, an approximately 1 mm crack was introduced at the notch tip by tapping a blade.[8,9] The results of the compact tension test were analyzed using Equation (2) from the ASTM D5045 to calculate the plane-strain fracture toughness, K_{I} in MPa $\text{m}^{0.5}$:

$$K_{\mathrm{I}} = \frac{\Delta P}{B\sqrt{W}} \times \frac{(2+\alpha)}{(1-\alpha)^{\frac{3}{2}}} \times \left(0.866 + 4.64\alpha - 13.32\alpha^2 + 14.72\alpha^3 - 5.6\alpha^4\right), \tag{2}$$

where ΔP is the difference between the highest and lowest load in megaNewton (MN), W and B are the sample's width and thickness, respectively, and α is the ratio of the crack length to the width of the sample.

2.4.2 | Scanning electron microscopy

A Tuscan MIRA3 FESEM (Czech Republic) was used to visualize the surface fracture of the composites broken after the tensile tests. Before testing, the samples were coated with a 12 nm thick layer of platinum to prevent charging.[36] Moreover, the scanning electron microscopy (SEM) was also used to determine the particle size of MCC and CNC dry powder where the samples were coated with a 10 nm layer of platinum before testing, and 20 particle size measurements were taken by image processing of the SEM software to calculate the average for each filler.

2.4.3 | Differential scanning calorimeter study

Q100 DSC (TA instruments-USA) was used to find the glass transition temperature of the composites and fillers in a heat/cool/heat mode between −50 and 200°C with a heating/cooling rate of 10°C/min. Differential scanning calorimeter (DSC) is a method that depends on variations in the heat flow to determine the glass transition temperature. The second heating cycle was used to determine the of the samples.[8,9]

2.4.4 | Dynamic mechanical analysis

DMA8000 (PerkinElmer) was used to analyze the dynamic and thermal properties of the MCC and CNC-based epoxy composites. This method depends on abrupt changes in the material's storage modulus as it shifts from glassy to rubbery to determine the glass transition temperature (T_{g}) and the damping factor (Tan D).[9] T_{g} and Tan D were determined from the onset temperature of the storage modulus versus temperature and the peak of Tan D curves, respectively. A single cantilever setup was required at a frequency of 1 Hz and a ramped temperature starting from 25 to 220°C at a 10°C/min rate. The samples were ground and polished to have a width of about 12 mm and a thickness of around 4 mm.

2.4.5 | Thermogravimetric analysis

Thermogravimetric analysis (TGA) Q500 (from TA Instruments, USA) was used to study the thermal stability of the composites and fillers. The composite of 7–15 mg was added to the pan inside the thermobalance of TGA and the temperature was raised from 25 to 800°C at a rate of 10°C/min under the nitrogen atmosphere.[8] From the resulting thermographs, the decomposition temperature (T_{d}) is determined from the onset temperature, the temperature where the maximum rate of weight loss occurs is $T_{\max}$, $T_{\max}$'s slope is $R_{\max}$, and the activation energy (Ea) is calculated based on the following equation:

$$\ln\left(\ln(1-\alpha)^{-1}\right) = Ea \times \frac{(T - T_{\max})}{R \times T_{\max}^2}, \tag{3}$$

where α is the decomposition ratio, R is the ideal gas constant, and T is the temperature in Kelvin. The activation energy is obtained from the slope of the plot of $\ln(\ln(1-\alpha)^{-1})$ versus $(T - T_{\max})$.[5]

3 | RESULTS AND DISCUSSION

3.1 | Filler characterization

3.1.1 | Crystallinity of MCC and CNCs

The Segal CI and the cellulose polymorphs of MCC and CNCs were evaluated via wide-angle x-ray scattering (WAXS) (Figure 4). As expected both, MCC and CNCs, illustrate a cellulose I pattern defined by the (1–10), (110), (200), and (004) peaks located at 2θ of 15°, 16°, 22°, and 34°.[35] The Segal CI % was found to be 74 ± 2% for MCC and 71 ± 1% for CNCs. These values are within the range of reported values in the literature achieved by the Segal, the peak height analysis method. The CI% values for MCC samples originated from cotton linters were found to be 72%–76% by Terinte et al.[37] Depending on the preparation method, CNCs are reaching CI in the range of 61%–85%.[38–41]

3.1.2 | Particle size analysis

SEM was used to determine the particle size of the CNC and MCC powders. Figure 5 shows the size and morphological difference between the CNC and MCC particles. As can be observed, CNC particles have irregular spherical shapes, whereas MCC particles have irregular long and sharp morphologies. MCC's long particle shape is an indication of its high aspect ratio. Furthermore, by having 20 different length measurements of the particles, the particle sizes of CNCs and MCC are 1.03 μm ± 0.21 and 18.56 μm ± 2.08, respectively.

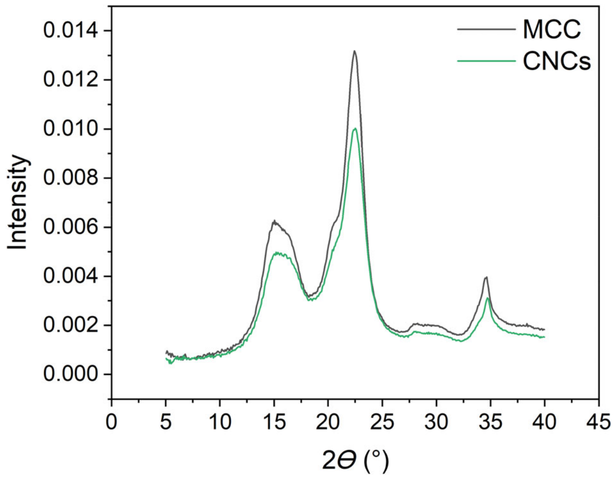

FIGURE 4 X-ray diffraction profiles of microcrystalline cellulose (black) and cellulose nanocrystals (green). [Color figure can be viewed at wileyonlinelibrary.com]

DLS analysis was also employed to measure the average particle size of MCC and CNC powders. Table 1 presents the particle size results of CNC and MCC powders at 0.5 wt% in water and ethanol. The results were in good agreement with the particle size reported by CelluForce when water was used for dispersing the particles.

In contrast with the DLS particle size measurements, SEM measurements on micrographic pictures analyze only a small fraction of particles, which offers a complementary perspective on particle size measurement.[42] Whereas DLS measurements are taken on a larger number of particles.[43] Nevertheless, the wet nature of the DLS test permits other types of limitations and errors in measurements such as when the measured material aggregates within the solvent and yields larger measurements than should be.[44] Moreover, other than measuring the particle size, SEM offers detailed shape and morphological information that are unique in comparison with the DLS.[43] The particle size analyses by DLS and SEM measurements have their advantages and limitations. Large particles quickly sediment from CNC/MCC dispersion and cannot be measured by DLS measurement while typically large particles and aggregates are observed by SEM. Overall, the particle size of CNC and MCC powders should be in the range of 100–1000 nm and 1.3–20 μm, respectively.

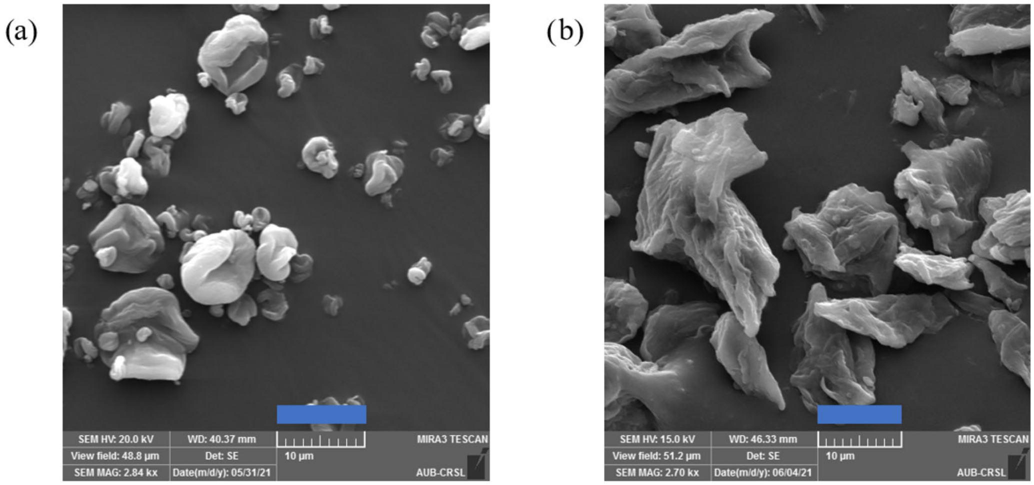

FIGURE 5 Scanning electron microscopy micrographs of (a) cellulose nanocrystal and (b) microcrystalline cellulose particles. [Color figure can be viewed at wileyonlinelibrary.com]

3.2 | Composite characterization

3.2.1 | Mechanical tensile testing

CNC/epoxy composites

Figure 6 shows the trend of tensile strength and elastic modulus as a function of pristine and dried CNC concentration. The values and error% have been collected in Table S1. As can be seen, the tensile strength of the composites can be enhanced by the addition of CNCs to a certain level. The maximum tensile strength of 45.7 MPa (corresponding to a 25% improvement) was achieved for the epoxy sample containing 2 wt% of pristine CNCs (not dried). When dried CNCs was used as a filler, the tensile strength of the resulting epoxy composite was enhanced and the maximum value of 56 MPa (corresponding to 54% improvement) was obtained at dried CNC content of 0.5 wt%. After this concentration, a gradual decrease in the tensile strengths of the composites was noticed, yet still performed better than pure epoxy. The elastic modulus of epoxy polymer without any filler was around 1005 MPa which was dropped to 923 MPa (corresponding to a −8% reduction). When dried CNC powder was used as a filler, the elastic modulus was impacted negatively even more and dropped to 820 MPa (corresponding to a −18% reduction).

TABLE 1 Dynamic light scattering particle size results.

0.5 wt% dispersion in water	**Average diameter (*D*) of 3 samples (nm)**
CNCs	139 ± 17
MCC	1356 ± 32
0.5 wt% dispersion in ethanol	
CNCs	534 ± 64
MCC	1346 ± 51

Abbreviations: CNCs, cellulose nanocrystal; MCC, microcrystalline cellulose.

Thus, the addition of CNC (pristine or dried) powders can increase the tensile strength of the resulting composites and reduce their elastic modulus. This is translated to the stronger epoxy composites that are more ductile. The decrease in the mechanical properties of the epoxy samples after a certain filler concentration can be due to their agglomeration in the matrix.[14] Our results clearly show the importance of filler water content on the mechanical properties of epoxy composites. The water content of CNC powder is interfering with the reaction of epoxy monomers with the hardeners and can end the polymerization reaction during the propagation phase. This important factor has been neglected in many previous papers on the mechanical properties of epoxy composites.

MCC/epoxy composites

The tensile properties of non-dried MCC-epoxy composites with different concentrations were obtained. The average values of tensile strength, strain, and modulus

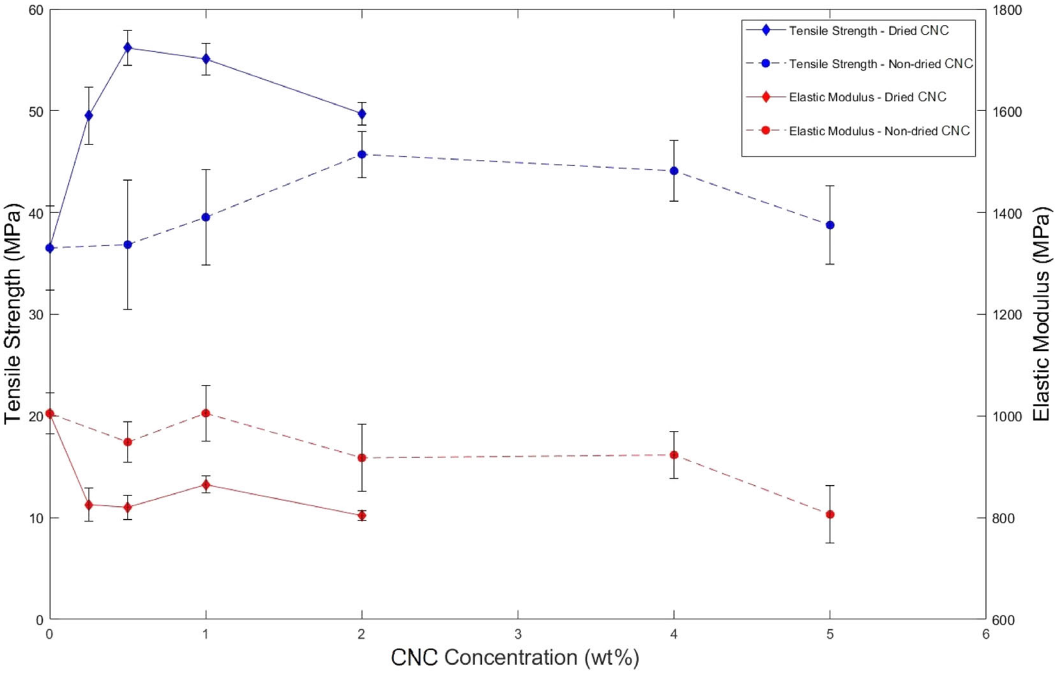

FIGURE 6 The tensile strength and elastic modulus of cellulose nanocrystal (CNC)-based epoxy composites for CNC powder before and after drying. [Color figure can be viewed at wileyonlinelibrary.com]

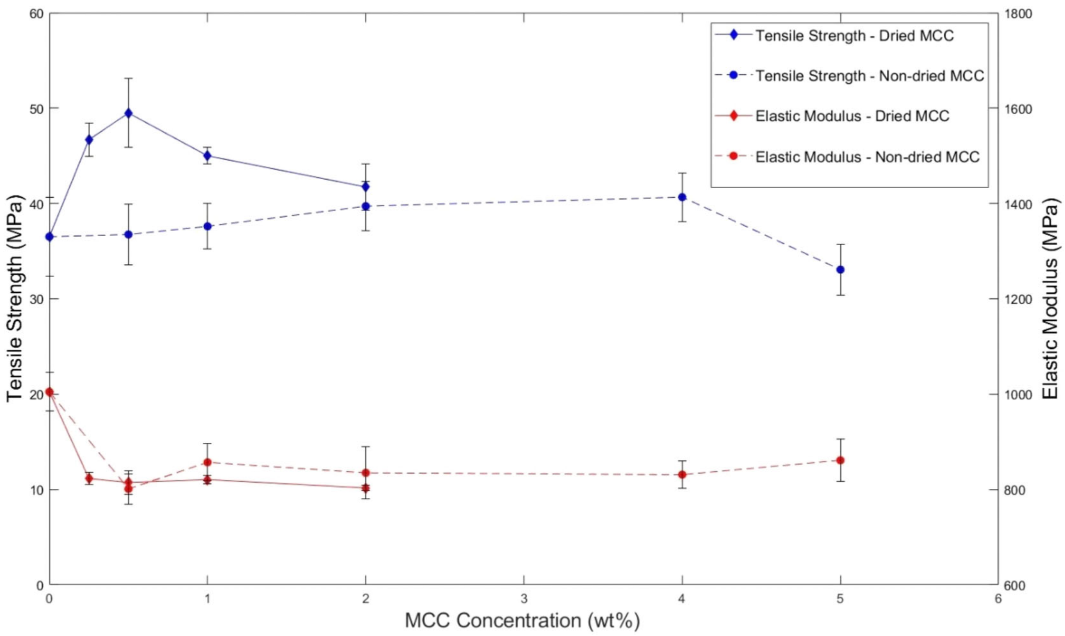

FIGURE 7 The tensile strength and elastic modulus of microcrystalline cellulose-based epoxy composites for cellulose nanocrystal powder before and after drying. [Color figure can be viewed at wileyonlinelibrary.com]

with their respective improvement percentage are reported in Table S2 and depicted in Figure 7.

Based on Figure 7, for all concentrations of MCC, an improvement was observed in the tensile strength of MCC-epoxy composites with the peak being at 49.5 MPa (corresponding to 35% improvement) at MCC 0.5 wt%. At higher dried MCC concentration, a decrease in the tensile was observed until it reached a value of 41.7 MPa at 2 wt% perhaps due to filler agglomeration in the matrix.

The elastic modulus of epoxy polymer without any filler was around 1005 MPa which was dropped to 835 MPa (corresponding to −17% reduction) at MCC 2 wt%. When dried MCC was used as a filler, the elastic modulus dropped to 814 MPa (corresponding to −19% reduction) at dried MCC 0.5 wt%.

By comparing the trend of tensile strength as a function of filler concentration for both MCC and CNC, we notice that CNC powder with a much lower particle size distribution can reinforce the epoxy composites better. The tensile strength of epoxy samples containing dried CNCs was between 49 and 56 MPa whereas that of the epoxy samples containing dried MCC remained between 41 and 49 MPa. This can be explained by the higher surface area to volume ratio of CNC particles and better interaction with the epoxy polymer matrix. The overall improvement in tensile strength comes from good and intimate adhesion and interaction between the polymer matrix and the filler, which allows for better stress transfer and imparts better mechanical properties. Epoxy composites reinforced with CNC and MCC displayed poorer mechanical properties (e.g., tensile strength) and diminishing benefits beyond 2 wt% CNC and MCC content. Post-drying, peak improvement occurred prior the 2 wt% threshold, making the pursue of point beyond 2 wt% less sought after. As we discussed in the previous section, drying the filler enhanced the mechanical properties such as the tensile strength of the epoxy composites within a certain range of filler content of up to 2 wt% for CNC and MCC. The moisture can destabilize the matrix–filler interface and cause de-bonding at the interface. Water also promotes inter- and intra-molecular hydrogen bonding between the water molecules and cellulosic fibers, leading to poor matrix–filler interaction.

3.2.2 | Compact tension testing

The fracture toughness K_I of the epoxy composites as a function of filler concentration has been provided in Figure 8. The average values and improvement % have been listed in Tables S3 and S4. With the addition of filler concentration, the fracture toughness of epoxy composites containing pristine MCC and CNC powders increased by 4%–5% and 4%–11%, respectively. The trend was somehow similar to that of tensile strength as a function of filler concentration. The fracture toughness of the epoxy composites containing dried CNCs was almost the same as those with pristine CNCs with no major changes in the trend. However, the fracture toughness of the samples containing dried MCC showed a slight

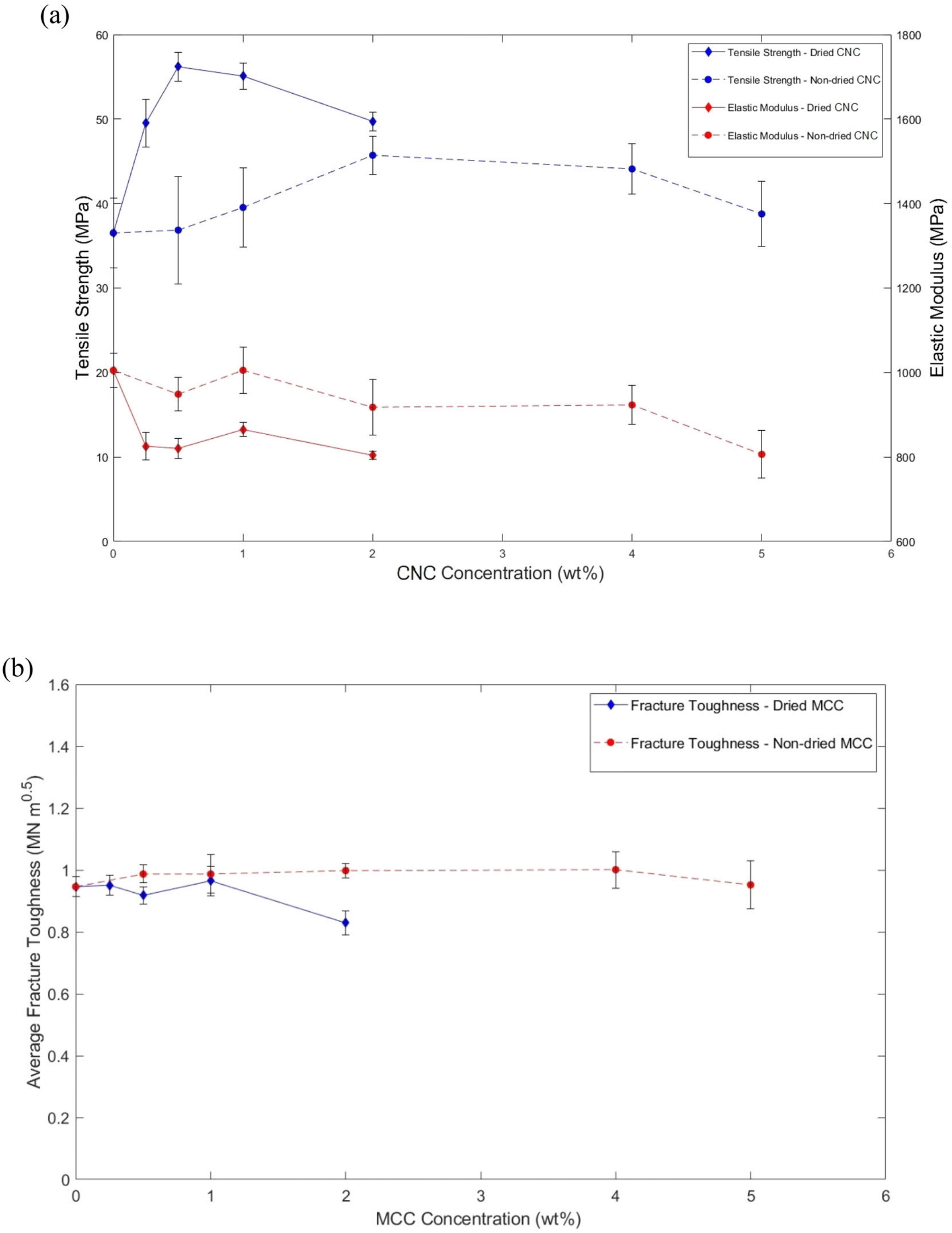

FIGURE 8 Fracture toughness of dried and non-dried (a) cellulose nanocrystal/epoxy and (b) microcrystalline cellulose/epoxy composites. [Color figure can be viewed at wileyonlinelibrary.com]

general decrease and dropped by −12% at MCC 2 wt%. The reported values are the average of several measurements and the general trend is in correlation with the trend of elastic modulus by the addition of the fillers.

For non-dried filler, the fracture toughness of pure epoxy was enhanced up to 5.6% at 4 wt% MCC/epoxy and up to 12% at 2 wt% CNC/epoxy. The trend was almost identical to that in the tensile tests, the fracture toughness increased gradually with the increase in concentration and then decreased at 5 wt% MCC/epoxy and 4 and 5 wt% in the case of CNC/epoxy composites. At a certain filler concentration, the fracture toughness of the composites decreases again, which is attributed to the agglomeration of the filler particles in the matrix, which act as stress points and facilitate the crack propagation.

The enhanced fracture toughness observed in the CNC-epoxy composites can be primarily attributed to the

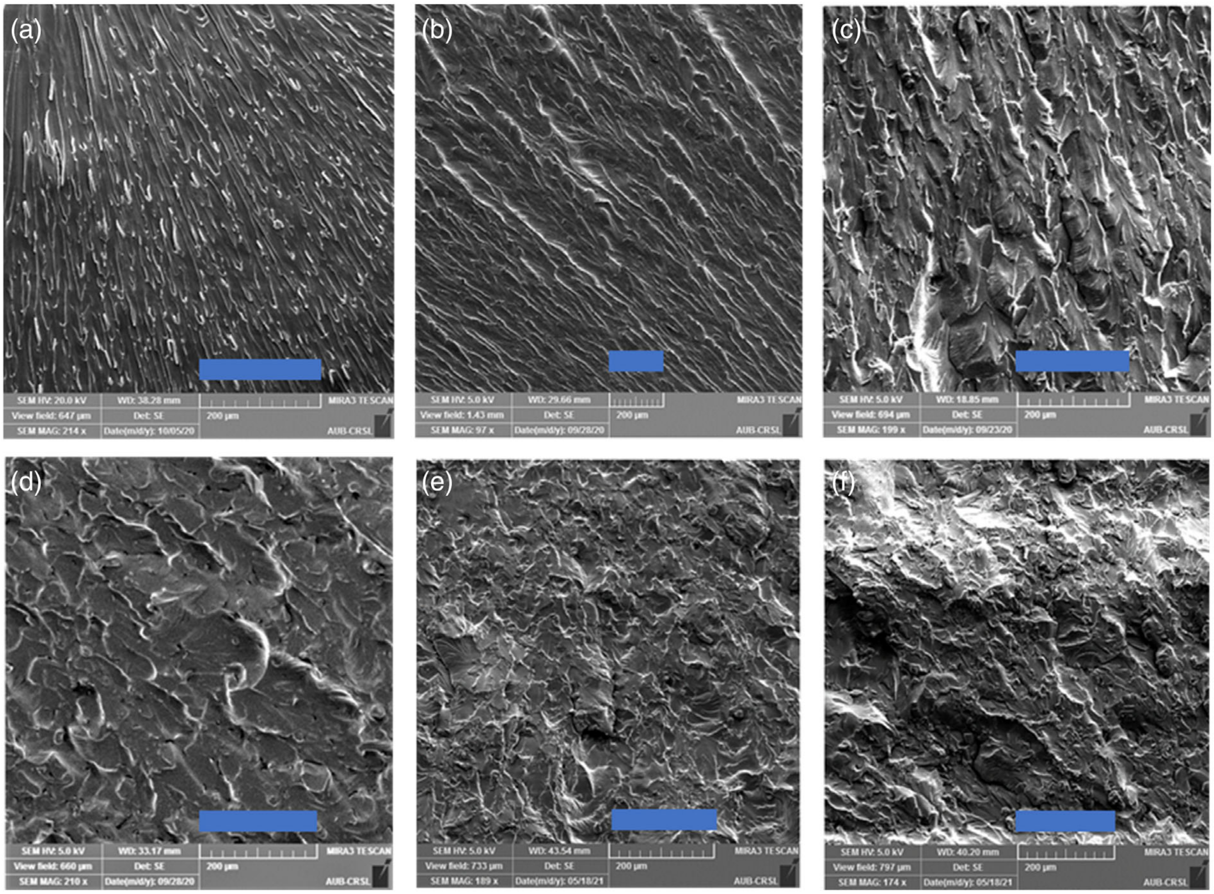

FIGURE 9 Fracture scanning electron microscopy images of cellulose nanocrystal (CNC)-epoxy composites at various concentrations of CNC powder: (a) 0.0 wt%, (b) 0.5 wt%, (c) 1 wt%, (d) 2 wt%, (e) 4 w.%, and (f) 5 wt%. The inserted blue scale-bars are 200 μm. [Color figure can be viewed at wileyonlinelibrary.com]

smaller size of CNC particles and their superior dispersion in the matrix. This advantageous combination allows the resulting composites to effectively resist the propagation of cracks, thereby improving their fracture toughness.

Based on the data presented in Figure 8, it can be observed that the fracture toughness values for both CNC- and MCC-epoxy composites fluctuated around the original value of the fracture toughness of pristine epoxy (0.956 MN m$^{0.5}$). Furthermore, the drying process of the filler did not significantly alter the fracture toughness of the composite materials in either case.

3.2.3 | SEM

To gain insight into the fracture behavior of the CNC- and MCC-based epoxy composites, SEM imaging of the fracture morphology was conducted following tensile testing. The obtained fracture images of the pure epoxy, CNC, and MCC-based epoxy composites are presented in Figures 9 and 10. It is evident from the SEM micrograph of the fractured pure epoxy sample that it exhibited typical brittle behavior, with the crack propagating smoothly in one direction. This observation is consistent with previous investigations.[16,45] With the addition of CNC or MCC powders, the crack propagation and trend lines widened part and the surface became rougher compared to that of pure epoxy. Bowing lines were observed as a result of crack pinning and deflection, which in turn decreased the propagation energy of the crack and increased the composites' strength and toughness.[8,9] Because of the presence of discontinuities in the materials (the reinforcement), as the crack is propagating and meets the discontinuity, the cracks deviates from their original direction and start to bow. The change in the propagation direction of the cracks consumes additional energy and mitigates the overall impact of the crack on the material's structural integrity. Hence, although cracks are present on the surface, their effect on the composite's strength is countered by the energy-absorbing mechanisms driven by the crack pinning and deflection, resulting in enhanced mechanical properties." However, beyond 2 wt% CNC and at 5 wt% MCC-epoxy composites,

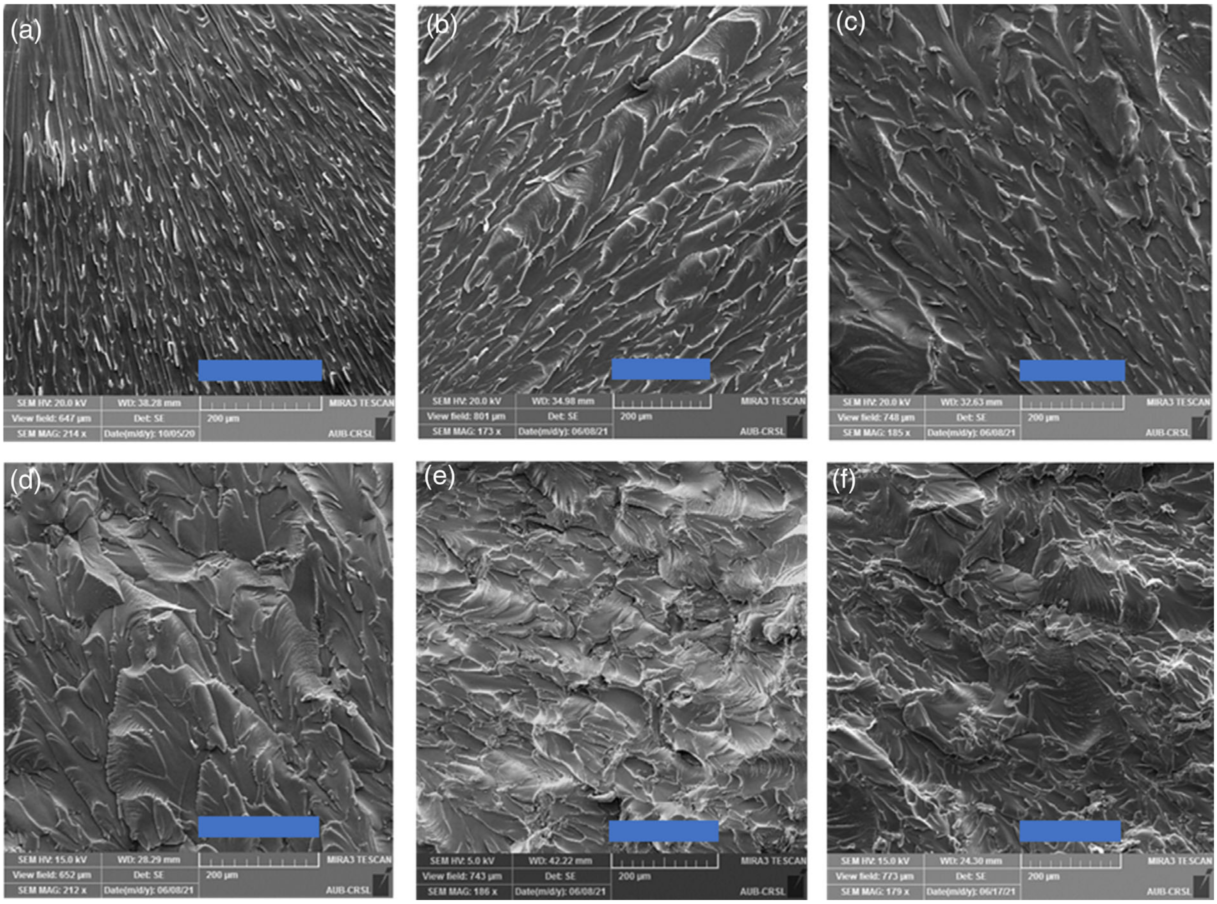

FIGURE 10 Fracture scanning electron microscopy images of microcrystalline cellulose (MCC)-epoxy composites at various concentrations of MCC: (a) 0.0 wt%, (b) 0.5 wt%, (c) 1 wt%, (d) 2 wt%, (e) 4 wt%, and (f) 5 wt%. The inserted blue scale-bars are 200 μm. [Color figure can be viewed at wileyonlinelibrary.com]

the trend lines became almost unrecognizable due to the significant deformations and evidence of clusters of particles observed in Figure 11. This confirmed the previous suggestion regarding the possibility of agglomeration, which deteriorated the composites' mechanical properties. Additionally, the large size of each MCC cluster in Figure 11 also can explain the sudden and significant degradation in the mechanical properties of the 5 wt% MCC/epoxy composite as it is not an unusual phenomenon and is evident in literature.[10]

With the addition of dried CNC and MCC powders, we observed more or less similar behavior to what is presented in Figures 9 and 10. The SEM micrographs of the fracture epoxy samples have been provided in Figure S1. Noticeable orientations and some distortions were observed in the surface cracks at low filler concentrations (less than 2 wt%). At higher concentrations, significant deformation was observed and crack trend lines became almost unrecognizable. At a certain filler concentration, filler agglomerates are observable in the SEM micrograph (Figure S2).

3.2.4 | DSC

The glass transition temperatures (T_g) of the different epoxy composites and their fillers were determined using DSC and the results are summarized in Table 2. The DSC thermograms of the pure epoxy, fillers, and CNC/MCC-epoxy composites are presented in Figure S3. The composites displayed complete curing behavior with no endothermic or exothermic peaks observed within the tested temperature range, indicating that they do not melt or decompose at these temperatures.[8,9]

The onset T_g of CNCs and MCC was found to be 142°C, explaining the slight increase in T_g observed for the composites containing 5 wt% of MCC and CNCs, which increased T_g from 134°C for the pure epoxy to 135.3 and 136.7°C for MCC- and CNC-epoxy composites, respectively. However, this change is negligible (1%–2%), suggesting that the addition of MCC or CNCs at up to 5 wt% does not significantly affect the thermal properties of pure epoxy. This conclusion was further supported by

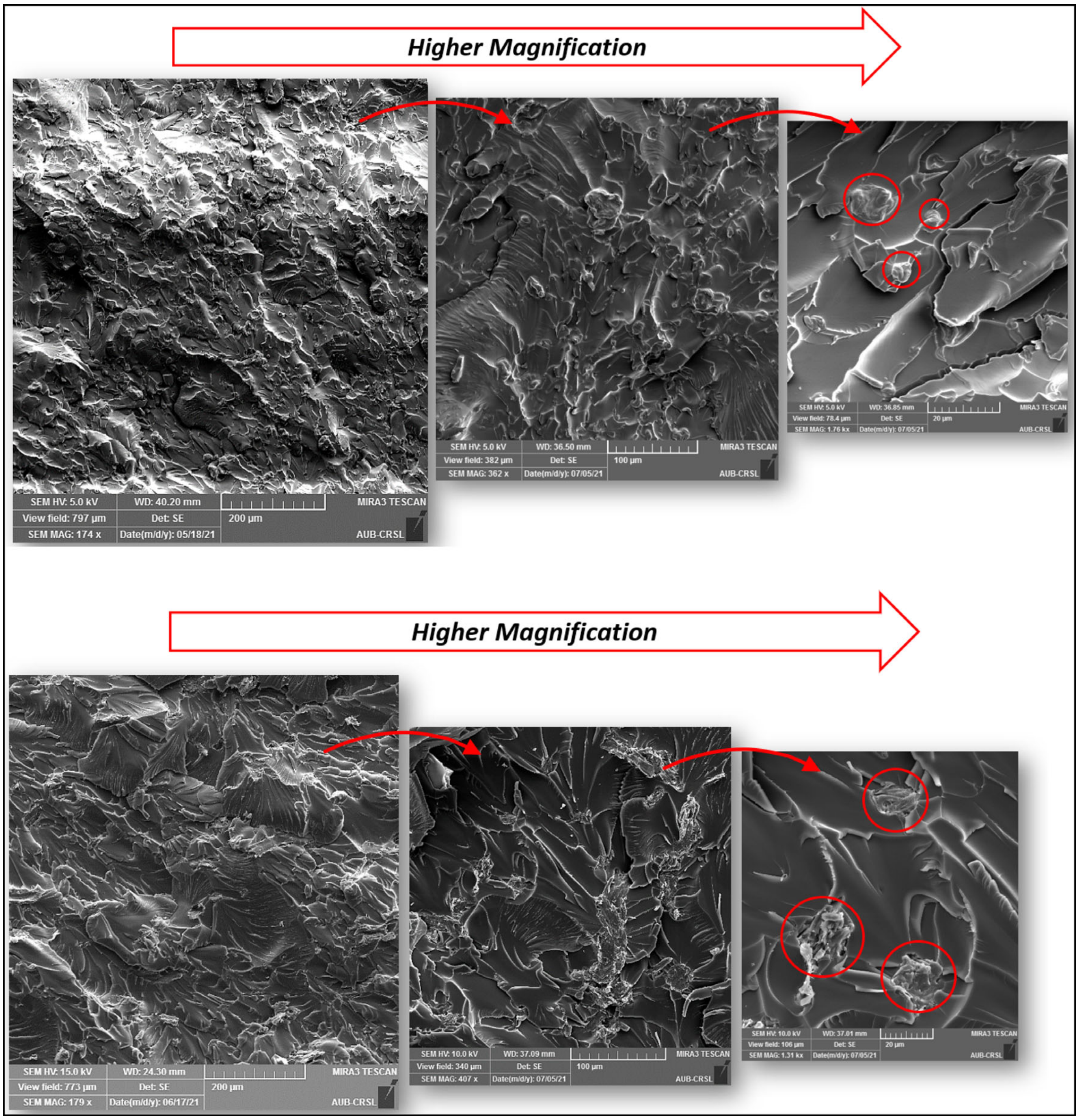

FIGURE 11 Sign of agglomeration at 5 wt% cellulose nanocrystal/epoxy composite (top) and 5 wt% microcrystalline cellulose/epoxy composite. [Color figure can be viewed at wileyonlinelibrary.com]

TABLE 2 Differential scanning calorimeter (DSC) results of microcrystalline cellulose (MCC) and cellulose nanocrystal (CNC)-epoxy composites.

DSC			DSC		
	Average onset T_g (°C)	Changes (%)		Average onset T_g (°C)	Changes (%)
Pure epoxy	134 ± 0.16	–	Pure epoxy	134 ± 0.16	–
0.5 wt% CNC	134.6 ± 0.73	0.46	0.5 wt% MCC	134 ± 0.55	0.04
1 wt% CNC	134.7 ± 0.89	0.56	1 wt% MCC	134.4 ± 0.18	0.35
2 wt% CNC	135.2 ± 0.91	0.92	2 wt% MCC	134.7 ± 0.79	0.55
4 wt% CNC	135.2 ± 0.85	0.94	4 wt% MCC	135.1 ± 0.52	0.84
5 wt% CNC	136.7 ± 2.45	2.01	5 wt% MCC	135.3 ± 0.86	1.02
CNC powder	142.67	–	MCC powder	142.17	–

TABLE 3 Dynamic mechanical analysis (DMA) results of microcrystalline cellulose (MCC) and cellulose nanocrystals (CNC)-epoxy composites.

DMA					
	Average onset T_g (°C)	**Average Tan *D***		**Average onset T_g (°C)**	**Average Tan *D***
Pure epoxy	159 ± 1.57	171 ± 0.98	Pure epoxy	159 ± 1.57	171 ± 0.98
0.5 wt% CNC	160 ± 3.57	171.4 ± 4.1	0.5 wt% MCC	159.4 ± 1.02	170.4 ± 4.29
1 wt% CNC	161.1 ± 4.33	171.8 ± 4.9	1 wt% MCC	159.5 ± 2.65	169.9 ± 4
2 wt% CNC	161.8 ± 0.87	172.2 ± 1.44	2 wt% MCC	159.6 ± 2.41	172.2 ± 4.1
4 wt% CNC	161.1 ± 5.2	171.3 ± 5.7	4 wt% MCC	159.6 ± 0.1	169.1 ± 0.85
5 wt% CNC	161.9 ± 1.04	172.3 ± 1.76	5 wt% MCC	160.4 ± 1.28	171.9 ± 1.06

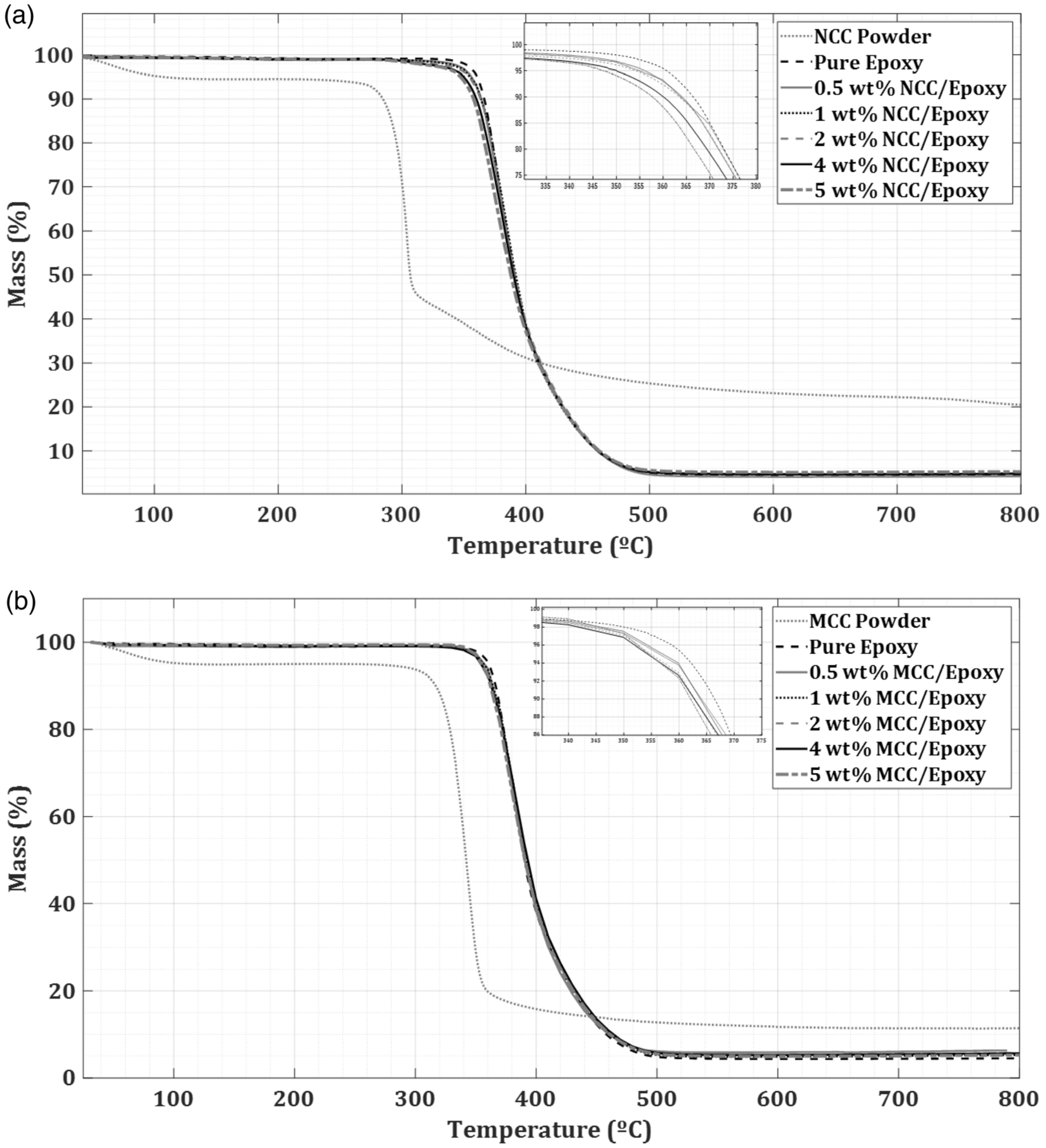

FIGURE 12 Thermogravimetric analysis thermographs of (a) cellulose nanocrystal (CNC)/epoxy and (b) microcrystalline cellulose (MCC)/epoxy composites including the thermographs of CNC and MCC powder.

the results of dynamic mechanical analysis (DMA) and confirmed by the TGA analysis of the epoxy composites.

3.2.5 | DMA

The glass transition temperatures of the different epoxy composites were studied by DMA. The storage modulus versus temperature profiles for MCC- and CNC-epoxy composites are presented in Figure S4. Accordingly, the onset T_g and the damping factor (Tan *D*) were calculated based on the profiles and reported in Table 3.

Similar to the DSC T_g results, the recorded T_g of the epoxy composites by the DMA showed a slight change. Pure epoxy which recorded a T_g of 159°C and Tan *D* of 171°C barely increased to T_g of 160–162°C and Tan *D* of 172°C as the concentration of CNCs and MCC increased till 5 wt%. The results show no chemical bond between the fillers and the epoxy matrix.

3.2.6 | TGA

To better understand how the addition of fillers affects the thermal stability of the final composites, the TGA was conducted on the different epoxy composites and fillers. The T_d, the temperature where the maximum rate of weight loss occurs (T_{max}), T_{max}'s slope (R_{max}), and the *E*a of the CNC and MCC/epoxy composites are determined from the thermograms presented in Figure 12 and are summarized in Table 4.

The thermographs of CNC and MCC powders displayed an initial weight loss in the range of 70–130°C. This initial weight loss (ca. 5%) can be related to the water content of the fillers that evaporates by heating. At temperatures higher than 200°C, the thermographs of CNC and MCC powders showed different thermal degradation behavior. The onset T_d of CNCs exhibited a value of 296.5°C, a lower value when compared with MCC's T_d of 330.2°C, as well as a higher residual value (20%) compared with MCC (11.4%). Moreover, MCC proved to be slightly more stable thermally than CNC powder due to its higher T_{max} (333.6°C compared with 304.5°C). According to the literature, this difference was explained by the fillers' different cellulose morphology that affected the resistance behavior to heat degradation.

Upon comparing MCC and CNCs, it was observed that CNCs had a higher number of free-end chains, which could be responsible for its decomposition at lower temperatures. As a result, CNCs generated a slightly higher amount of residue compared with MCC.[46,47] Furthermore, the difference in the T_d values of the fillers and pure epoxy can also explain the slight decrease trend in the T_d results of the composites as filler content increased. The decomposition profiles of the CNC and MCC/epoxy composites were similar such that the addition of CNC or MCC particles up to 5 wt% slightly decreased the T_d to 358 and 360°C, respectively. This decrease was also observed in T_{max}, inversely proportional to its slope R_{max}. Nevertheless, no significant residual change was observed, which can be attributed to the low concentration of fillers added (0.5%–5%) as well as the fact that the fillers used are organic materials that

TABLE 4 Thermogravimetric analysis (TGA) results of microcrystalline cellulose (MCC) and cellulose nanocrystal (CNC)-epoxy composites and fillers.

TGA	Average residue (%) at 800°C	Average T_d (°C)	T_{max} (°C)	R_{max} (%/°C)	Ea (kJ/mol)
Pure epoxy	4.9	362.1 ± 0.9	391.4	−2.66	−23.5
0.5 wt% CNC	4.5	359.8 ± 0.4	383.9	−1.961	−23.06
1 wt% CNC	4.9	360.1 ± 0.7	381.5	−1.679	−21.74
2 wt% CNC	4.6	360.6 ± 0.8	381	−1.678	−22.05
4 wt% CNC	4.9	359.2 ± 0.1	375.3	−1.61	−22.03
5 wt% CNC	5.4	358.0 ± 0.7	372.7	−1.5	−21.5
0.5 wt% MCC	6	362.1 ± 0.3	381.5	−1.615	−22.8
1 wt% MCC	5.5	361.5 ± 0.5	380.8	−1.624	−21.34
2 wt% MCC	5.3	360.8 ± 0.8	381.1	−1.657	−21.35
4 wt% MCC	5.7	360.4 ± 0.9	379.9	−1.597	−21.28
5 wt% MCC	5.3	359.8 ± 0.8	378.1	−1.579	−21.16
CNC powder (15.7 mg)	20	296.2	304.5	−1.62	−12.5
MCC powder (12.7 mg)	11.4	330.2	333.6	−1.71	−15.3

decompose at around 315°C. Thus, at 800°C barely any additional residue to that of pure epoxy would remain. Considering no significant change in *E*a values of epoxy composites, there should be very weak bonding between the filler and epoxy matrix and no enhancement of thermal stability.[48] This can be explained by the low concentration of MCC and CNC powders with their lower degradation temperature.

4 | CONCLUSIONS

The goal of this study is to reinforce epoxy composites by adding MCC and CNC powders. We studied the effect of filler particle size, filler concentration, and moisture content on the thermo-mechanical properties of epoxy composites. The results can be summarized as follows:

CNC-reinforced epoxy composites showed somewhat better tensile strength than MCC-reinforced epoxy composites at optimum filler concentration. This is attributed to the better dispersion and adhesion of CNCs in the polymer matrix due to their lower particle size distribution and higher surface area-to-volume ratio.

The tensile strength of the epoxy-based composite increased with the addition of pristine MCC or CNCs to a certain level. The maximum tensile strength of the CNC-epoxy composites at 2 wt% CNC was found to be 45 MPa (corresponding to 25% enhancement) and the maximum tensile strength of MCC-epoxy composites at 4 wt% MCC was obtained to be 41 MPa (corresponding to 11.4% improvement). At higher filler concentrations, the tensile strength dropped again probably due to the filler agglomeration and their lower interfacial interactions at the polymer matrix/filler boundary.

When dried fillers were used for the preparation of epoxy composites, the maximum tensile strength of CNC-epoxy and MCC-epoxy composites at 0.5 wt% dried-filler was found to be 56 MPa (53.8% enhancement) and 49.5 MPa (35.5% enhancement), respectively. Hence, epoxy composites with higher tensile strength values can be obtained at much lower dried filler concentrations, which is important from an economic point of view.

The SEM micrographs showed recognizable filler agglomeration at high filler concentrations (e.g., 4 and 5 wt% CNCs and MCC). Despite some distortions in the crack morphology, crack orientations were still noticeable in some cases.

The fracture toughness of MCC-epoxy composites enhances by 4%–5% at MCC concentration 1–4 wt%. The fracture toughness of CNC-epoxy samples increased by 4.7%–11% at CNC initial concentration between 1 and 5 wt%. We did not observe a clear trend for the fracture toughness of the epoxy composites reinforced with dried MMC or CNCs.

The results of DSC, DMA, and TGA did not show any significant differences between the epoxy composites with or without fillers. So, the thermal behavior of the epoxy composites is not affected by the addition of MCC or CNCs at low initial concentrations of 1–5 wt%.

AUTHOR CONTRIBUTIONS

Patricia Semaan: Formal analysis (equal); investigation (equal); methodology (equal); writing – original draft (equal). **Abraham Zahran:** Formal analysis (equal); investigation (equal); methodology (equal); writing – original draft (equal). **Inge Schlapp-Hackl:** Formal analysis (supporting); investigation (supporting); writing – review and editing (supporting). **Samir Mustapha:** Conceptualization (equal); project administration (equal); supervision (equal); writing – review and editing (equal). **Ali R. Tehrani-Bagha:** Conceptualization (equal); project administration (equal); supervision (equal); writing – review and editing (equal).

ACKNOWLEDGMENTS

Scanning electron microscopy and dynamic light scattering analyses were performed using equipment and facilities in the Kamal A. Shair Central Research Science Laboratory at the American University of Beirut.

FUNDING INFORMATION

The authors acknowledge the financial support of the University Research Board at the American University of Beirut for their Award # 104260.

CONFLICT OF INTEREST STATEMENT

The authors have no competing interests as defined by Springer, or other interests that might be perceived to influence the results and/or discussion reported in this paper.

DATA AVAILABILITY STATEMENT

The data and materials may be obtained from authors upon request.

ORCID

Ali R. Tehrani-Bagha https://orcid.org/0000-0002-8206-3827

REFERENCES

[1] I. O. Oladele, T. F. Omotosho, A. A. Adediran, *Int. J. Polym. Sci.* **2020**, *2020*, 8834518. https://doi.org/10.1155/2020/8834518

[2] V. Dhinakaran, K. V. Surendar, M. S. Hasunfur Riyaz, M. Ravichandran, *Mater. Today: Proc.* **2020**, *27*, 812.

[3] J.-P. Pascault, R. J. J. Williams Eds., *Epoxy Polymers: New Materials and Innovations*, Wiley, Hoboken, USA, **2010**.

[4] I. Rafique, A. Kausar, B. Muhammad, *Polym.-Plast. Technol. Eng.* **2016**, *55*, 1653.

[5] A. A. Tarhini, A. R. Tehrani-Bagha, *Compos. Sci. Technol.* **2019**, *184*, 107797.

[6] A. Tarhini, A. Tehrani-Bagha, M. Kazan, B. Grady, *J. Appl. Polym. Sci.* **2021**, *138*, 49821. https://doi.org/10.1002/app.49821

[7] M. D. Kiran, H. K. Govindaraju, T. Jayaraju, N. Kumar, *Mater. Today-Proc.* **2018**, *5*, 22421.

[8] Y. N. Baghdadi, L. Youssef, K. Bouhadir, M. Harb, S. Mustapha, D. Patra, A. R. Tehrani-Bagha, *J. Appl. Polym. Sci.* **2020**, *137*, 49330. https://doi.org/10.1002/app.49330

[9] Y. N. Baghdadi, L. Youssef, K. Bouhadir, M. Harb, S. Mustapha, D. Patra, A. R. Tehrani-Bagha, *J. Appl. Polym. Sci.* **2021**, *138*, 50533. https://doi.org/10.1002/app.50533

[10] Y. N. Baghdadi, J. Sinno, K. Bouhadir, M. Harb, S. Mustapha, D. Patra, A. R. Tehrani-Bagha, *J. Appl. Polym. Sci.* **2021**, *138*, 51324. https://doi.org/10.1002/app.51324

[11] F. A. Dos Santos, G. C. V. Iulianelli, M. I. B. Tavares, *Polym. Test.* **2017**, *61*, 280.

[12] W. Y. Hamad, *Cellulose Nanocrystals: Properties, Production and Applications*, Wiley, Hoboken, USA, **2017**, p. 312.

[13] C. Miao, W. Y. Hamad, *Curr. Opin. Solid State Mater. Sci.* **2019**, *23*, 100761.

[14] X. Xu, F. Liu, L. Jiang, J. Y. Zhu, D. Haagenson, D. P. Wiesenborn, *ACS Appl. Mater. Interfaces* **2013**, *5*, 2999.

[15] H. Seok, D. S. Kim, *Polym. Eng. Sci.* **2020**, *60*, 439, https://doi.org/10.1016/j.rineng.2022.100842

[16] A. Kiziltas, D. J. Gardner, Y. Han, H.-S. Yang, *J. Polym. Environ.* **2014**, *22*, 365.

[17] S. A. Awad, S. S. Mahini, S. J. Tucker, C. M. Fellows, *Int. J. Polym. Anal. Charact.* **2019**, *24*, 150.

[18] T. Aziz, H. Fan, X. Zhang, F. U. Khan, *Mater. Res. Express* **2019**, *6*, 1150b7. https://doi.org/10.1088/2053-1591/ab4df6

[19] H.-Y. Yu, J.-M. Yao, *Compos. Sci. Technol.* **2016**, *136*, 53.

[20] E. Fortunati, I. Armentano, Q. Zhou, D. Puglia, A. Terenzi, L. A. Berglund, J. M. Kenny, *Polym. Degrad. Stab.* **2012**, *97*, 2027.

[21] X. E. Xiao, S. R. Lu, B. Qi, C. Zeng, Z. K. Yuan, J. H. Yu, *Rsc Adv.* **2014**, *4*, 14928.

[22] S. X. Peng, R. J. Moon, J. P. Youngblood, *Green Mater.* **2014**, *2*, 193.

[23] W. Lixin, H. Suong, T. Minh-Tan, *J. Appl. Polym. Sci.* **2004**, *92*, 2261.

[24] N. Sharp, C. Li, A. Strachan, D. Adams, R. Byron Pipes, *J. Polym. Sci.* **2017**, *55*, 1150.

[25] R. Cruz, L. Correia, S. Cabral-Fonseca, J. Sena-Cruz, *Int. J. Adhes. Adhes.* **2021**, *110*, 102961.

[26] T. Kumazawa, M. Oishi, M. Todoki, *IEEE Trans. Dielectr. Electr. Insul.* **1994**, *1*, 133.

[27] G. Quino, V. Tagarielli, N. Petrinic, *Compos. Sci. Technol.* **2020**, *199*, 108316.

[28] B. M. Trinh, T. Mekonnen, *Polymer* **2018**, *155*, 64.

[29] T. Aziz, H. Fan, X. Zhang, F. U. Khan, S. Fahad, A. Ullah, *J. Polym. Eng.* **2020**, *40*, 314.

[30] S. Pruksawan, S. Samitsu, Y. Fujii, N. Torikai, M. Nato, *Appl. Polym. Mater.* **2020**, *2*, 1234.

[31] E. Abraham, D. Kam, Y. Nevo, R. Slattegard, A. Rivkin, S. Lapidot, O. Shoseyov, *Appl. Mater. Interfaces* **2016**, *8*, 28086.

[32] M. Y. Rivera Lopez, J. M. Lambas, J. P. Stacey, S. Gamage, A. Suliga, A. Viquerat, F. Scarpa, I. Hamerton, *Molecules* **2020**, *25*, 1483. https://doi.org/10.3390/molecules25071483

[33] R. A. May, K. J. Stevenson, *Software review of Origin*, Vol. 131, American Chemical Society Publications, **2009**, *8*, p. 872.

[34] S. Nam, A. D. French, B. D. Condon, M. Concha, *Carbohydr. Polym.* **2016**, *135*, 1.

[35] A. J. Kinloch, X. Deng, S. Pimenta, G. T. Schueneman, S. Sprenger, A. C. Taylor, W. S. Teo, Homogeneous and toughened cellulose epoxy composites. Available: https://www.scopus.com/record/display.uri?eid=2-s2.0-85053134076&origin=resultslist&sort=plf-f&src=s&st1=Taylor&st2=Ambrose&nlo=1&nlr=20&nls=count-f&sid=0d22a4bd316418013426cbbbd6e49bc5&sot=anl&sdt=sisr&sl=38&s=AU-ID%28%22Taylor%2c+Ambrose+C.%22+8950608200%29&ref=%28cellulose%29&relpos=4&citeCnt=4&searchTerm= (accessed: August 2017).

[36] N. Terinte, R. Ibbett, K. C. Schuster, *Lenzinger Ber.* **2011**, *89*, 118.

[37] N.-M. Park, S. Choi, J. E. Oh, D. Y. Hwang, *Carbohydr. Polym.* **2019**, *223*, 115114.

[38] Y. Li, Y. Liu, W. Chen, Q. Wang, Y. Liu, J. Li, H. Yu, *Green Chem.* **2016**, *18*, 1010.

[39] M. Lee, M. H. Heo, H. Lee, H. H. Lee, H. Jeong, Y. W. Kim, J. Shin, *Green Chem.* **2018**, *20*, 2596.

[40] H. J. Kim, W. J. Lee, *Materials* **2023**, *16*, 2323.

[41] Y. Boluk, C. Danumah, *J. Nanopart. Res.* **2013**, *16*, 2174. https://doi.org/10.1007/s11051-013-2174-4

[42] A. Bootz, V. Vogel, D. Schubert, J. Kreuter, *Eur. J. Pharm. Biopharm.* **2004**, *57*, 369.

[43] D. Viet, S. Beck-Candanedo, D. G. Gray, *Cellulose* **2006**, *14*, 109.

[44] Y. Liu, Y. Wang, C. Zhang, T. Liu, *APL Mater.* **2019**, *7*, 080904-1. https://doi.org/10.1063/1.5110228

[45] E. Zeinali, V. Haddadi-Asl, H. Roghani-Mamaqani, *RSC Adv.* **2014**, *4*, 31428.

[46] L. K. Kian, M. Jawaid, *Int. J. Innov. Technol. Explor. Eng.* **2019**, *9*, 5430.

[47] N. D. Ahmad, Kusmono, M. W. Wildan, Herianto, Preparation and properties of cellulose nanocrystals-reinforced Poly (lactic acid) composite filaments for 3D printing applications, Results in Engineering, **2023**, 17.

[48] E. Sadeghpour, H. Wang, Y. Guo, D. H. C. Chua, V. P. W. Shim, *Composites Part A* **2020**, *129*, 105729.

SUPPORTING INFORMATION

Additional supporting information can be found online in the Supporting Information section at the end of this article.

How to cite this article: P. Semaan, A. Zahran, I. Schlapp-Hackl, A. R. Tehrani-Bagha, S. Mustapha, *J. Appl. Polym. Sci.* **2024**, *141*(14), e55180. https://doi.org/10.1002/app.55180